AD-A136 257 UNSTEADY BOUNDARY LAYERS ON THIN BODIES OF REVOLUTION 1/1
(U) MCDONNELL DOUGLAS CORP LONG BEACH CA
T CEBECI ET AL. AUG 83 AFOSR-TR-83-1211
UNCLASSIFIED F49620-82-C-0055 F/G 20/4 NL

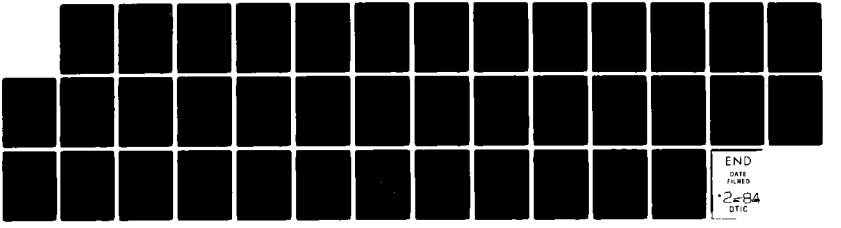

END
DATE FILMED
2-84
DTIC

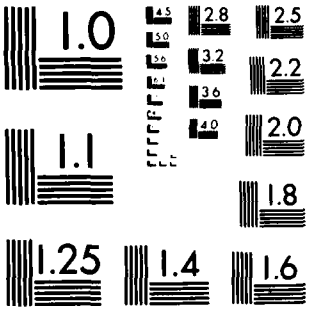

MICROCOPY RESOLUTION TEST CHART
NATIONAL BUREAU OF STANDARDS 1963 A

UNSTEADY BOUNDARY LAYERS ON THIN BODIES OF REVOLUTION

by

Tuncer Cebeci*, Keith Stewartson**, and Suzanne M. Schimke*

Abstract

The evolution of unsteady boundary layers on the line of symmetry of a thin prolate spheroid in uniform motion at constant angle of attack after an impulsive start is studied for a prescribed pressure distribution and results have been obtained for angles of attack ranging from 30° to 50°. The study shows that if $\alpha < \alpha_c (\simeq 41°)$ and the steady-state boundary layer exists everywhere on this line of symmetry, the unsteady solution approaches its steady-state solution rapidly without any significant special features. The same is true for $\alpha < \alpha_c$ on the windward side: on the leeward side, however, the steady-state boundary layer separates and the solution terminates. The unsteady boundary layer is initially unseparated but develops a region of reversed flow after a finite time. A short time later, the streamwise displacement thickness develops a pronounced peak and leads to a singularity of the same type as that observed by van Dommelen and Shen on a circular cylinder started impulsively from rest.

1.0 INTRODUCTION

Our knowledge of unsteady boundary layers has been enhanced in recent years by a combination of experimental and computational investigations. The former have been concerned mainly with the problem of airfoils which oscillate in subsonic flows but include a small number of transonic flow investigations.

*Aerodynamics Research & Technology, Douglas Aircraft Company, Long Beach, CA.

**Deceased; formerly Department of Mathematics, University College, London.

UNCLASSIFIED

SECURITY CLASSIFICATION OF THIS PAGE

REPORT DOCUMENTATION PAGE

1a. REPORT SECURITY CLASSIFICATION Unclassified	1b. RESTRICTIVE MARKINGS
2a. SECURITY CLASSIFICATION AUTHORITY	3. DISTRIBUTION/AVAILABILITY OF REPORT Approved for Public Release; Distribution Unlimited.
2b. DECLASSIFICATION/DOWNGRADING SCHEDULE	
4. PERFORMING ORGANIZATION REPORT NUMBER(S)	5. MONITORING ORGANIZATION REPORT NUMBER(S) AFOSR-TR- 83-1211
6a. NAME OF PERFORMING ORGANIZATION MCDONNELL DOUGLAS CORPORATION 6b. OFFICE SYMBOL (If applicable)	7a. NAME OF MONITORING ORGANIZATION
6c. ADDRESS (City, State and ZIP Code) 3855 LAKEWOOD BOULEVARD LONG BEACH, CA 90846	7b. ADDRESS (City, State and ZIP Code)
8a. NAME OF FUNDING/SPONSORING ORGANIZATION AIR FORCE OFFICE OF SCIENTIFIC RESEARCH 8b. OFFICE SYMBOL (If applicable) AFOSR/NA	9. PROCUREMENT INSTRUMENT IDENTIFICATION NUMBER F49620-82-C-0055
8c. ADDRESS (City, State and ZIP Code) BOLLING AFB, DC 20332	10. SOURCE OF FUNDING NOS. PROGRAM ELEMENT NO. 61102F; PROJECT NO. 2307; TASK NO. K1; WORK UNIT NO.
11. TITLE (Include Security Classification) UNSTEADY BOUNDARY LAYERS ON THIN BODIES OF REVOLUTION (UNCLASSIFIED)	
12. PERSONAL AUTHOR(S) TUNCER CEBECI KEITH STEWARTSON SUZANNE M SCHIMKE	
13a. TYPE OF REPORT Technical 13b. TIME COVERED FROM _____ TO _____	14. DATE OF REPORT (Yr., Mo., Day) 1983, August 15. PAGE COUNT 37
16. SUPPLEMENTARY NOTATION	

17. COSATI CODES			18. SUBJECT TERMS (Continue on reverse if necessary and identify by block number)
FIELD	GROUP	SUB. GR.	
			FLUID MECHANICS; BOUNDARY LAYER SEPARATION
			BOUNDARY LAYERS; INTERACTIVE BOUNDARY LAYERS
			UNSTEADY FLOWS; BODIES OF REVOLUTION - AERODYNAMICS

19. ABSTRACT (Continue on reverse if necessary and identify by block number)

The evolution of unsteady boundary layers on the line of symmetry of a thin prolate spheroid in uniform motion at constant angle of attack after an impulsive start is studied for a prescribed pressure distribution and results have been obtained for angles of attack ranging from 30° to 50°. The study shows that if $\alpha < \alpha_c$ ($\alpha_c \approx 41^{\circ}$) and the steady-state boundary layer exists everywhere on this line of symmetry, the unsteady solution approaches its steady-state solution rapidly without any significant special features. The same is true for $\alpha < \alpha_c$ on the windward side: on the leeward side, however, the steady-state boundary layer separates and the solution terminates. The unsteady boundary layer is initially unseparated but develops a region of reversed flow after a finite time. A short time later, the streamwise displacement thickness develops a pronounced peak and leads to a singularity of the same type as that observed by van Dommelen and Shen on a circular cylinder started impulsively from rest.

20. DISTRIBUTION/AVAILABILITY OF ABSTRACT UNCLASSIFIED/UNLIMITED ☒ SAME AS RPT. ☐ DTIC USERS ☐	21. ABSTRACT SECURITY CLASSIFICATION UNCLASSIFIED
22a. NAME OF RESPONSIBLE INDIVIDUAL Michael S Francis, Capt, USAF	22b. TELEPHONE NUMBER (Include Area Code) 202/767-4935 22c. OFFICE SYMBOL AFOSR/NA

DD FORM 1473, 83 APR EDITION OF 1 JAN 73 IS OBSOLETE.

UNCLASSIFIED

SECURITY CLASSIFICATION OF THIS PAGE

The latter have involved the solution of boundary-layer equations for flows over cylinders and airfoils and have been concerned largely with the nature of the singularity which occurs near separation. Solutions of the Navier-Stokes equations have also been obtained to provide an overall understanding of the flow patterns at conditions near or at dynamic stall. Useful reviews of previous work have been provided by Telionis (1979), McCroskey (1982), Williams (1977) and Cebeci (1982).

The experimental investigations have been carried out mainly to improve understanding of flow around helicopter rotor blades and include the low-speed measurements of McCroskey et al. (1982), Carr et al. (1977), Carr and McAlister (1983), Young (1982), Geissler (1983) and Cousteix et al. (1981) and transonic flow measurements of Davis and Malcolm (1980) and Dowell et al. (1981). The range of measurements of McCroskey et al. and Carr et al., in particular, is extensive and includes more than fifty combinations of Mach number and parameters of the unsteady motion for each of eight airfoil sections. As a consequence, four flow regimes have been identified and correspond to no stall, stall onset, light stall and deep stall. It appears that the breakdown of the unsteady boundary layer leads to a large vortex which is formed near the surface at large angles of attack and causes stall to occur shortly thereafter.

Computational investigations of oscillating airfoil flows have been of two main types. In the first, solutions of the Navier-Stokes equations have been obtained, for example by Mehta (1977) for incompressible laminar flows and by Shamroth (1981) for compressible turbulent flows. Further studies of this type are clearly necessary and results so far show qualitative features of the flow field and lift curves which are again in qualitative agreement with experiment. The second approach has involved the solution of the boundary-layer equations. The investigations of Cebeci and Carr (1981, 1983) have reported results for an external velocity distribution typical of those found near the leading edge of thin airfoils. The existence of a singularity in the

solutions is evident in the vicinity of the leading edge at the higher angles of attack and has led to the subsequent investigations of its nature, see for example, Cebeci, et al. (1983).

The need for more fundamental investigations of the use of boundary-layer equations to represent unsteady flows is clear from the airfoil investigations of the previous paragraph. In this connection, the oscillating flat plate investigations of Cousteix et al. (1981) and the contributions of Telionis (1974), van Dommelen and Shen (1982), Smith (1982) and Cebeci (1979, 1982) for flow over a cylinder impulsively started from rest are particularly relevant. In addition, Williams (1982) and Williams and Stewartson (1983) have made important contributions to our understanding of the nature of the singularity and its consequences. Perhaps the most important contribution has been that of van Dommelen and Shen (1982a) who solved the boundary-layer equations in Lagrangian form and revealed the existence of the singularity. This result suggests the need for interaction between the viscous and inviscid flow equations.

Though a number of studies have been conducted to improve our understanding of unsteady two-dimensional boundary layers, very little work has been done for unsteady three-dimensional flows. Experimental information is lacking, but the similarity between the two- and three-dimensional equations suggests that the same phenomena may occur. The three-dimensional boundary layer on a body of revolution at angle of attack is obviously more complicated than for airfoils or cylinders but is similar on the line of symmetry, provided that cross-flow gradients are taken into account. In the case of steady flow past thin spheroids, it is known [see Cebeci et al. 1981a] that separation does not occur on the leeward side until well past the maximum thickness if the angle of attack α is less than a critical value $\alpha_c (\simeq 41°)$, but for $\alpha > \alpha_c$ there is a dramatic change with separation occurring very close to the nose. If the

external velocity is prescribed, this abruptly terminates the integration. For thin airfoils there is a parallel situation but the critical angle is now of the order of magnitude of the airfoil thickness.

In this paper we report a study of the unsteady boundary layer on the line of symmetry to determine the relation between unsteady separation and singularities in the solution. For the first step we concentrate on the separation problem and do not consider the effect of moving stagnation points which is important but adds considerably to the computational difficulties. The particular problem we study is the development of a boundary layer on a thin spheroid in uniform motion at constant angle of attack after an impulsive start. Angles of attack ranging from 30° to 50° are chosen for this purpose. Of these $\alpha = 45°$ corresponds to nose separation which is marginal while $\alpha = 50°$ corresponds to a strong steady-state singularity. The problem has been formulated for the general case of spheroids at angles of attack and specialized to thin bodies, and specifically those for which the thickness ratio τ is vanishingly small.

2.0 APPROACH

With respect to a cylindrical-polar set of coordinates (x,r,θ) and origin O, let the equation of the spheroid be

$$\tau^2 x^2 + r^2 = \tau^2 \qquad (1)$$

where τ is a positive number less than unity, which may be regarded as a measure of the thickness ratio of the prolate spheroid. Here we have nondimensionalized the coordinates and time t taking the semi-major axis and the velocity at infinity to be unity. We assume that at an infinite distance from the spheroid the velocity of the fluid is in a direction lying in the meridional plane $\theta = 0$ and making an angle α with its major axis. Further we assume that outside the boundary layer the inviscid flow is irrotational and

attached and neglect the circulation around the spheroid. Although the circulation is generally important, particularly at large angles of attack, near the nose its effect is mainly to change the value of α and so the general conclusions of this investigation may be modified to take account of it in defining α in terms of the position of the forward stagnation point. The achievement of our goal of determining the development of the boundary layer, given the main-stream velocity, would be an important step forward in the task of predicting the circulation around bodies of revolution at incidence.

With these assumptions the velocity of slip on the spheroid, according to inviscid theory, has components

$$\begin{aligned} u_e &= V_0(\tau)\cos\alpha\cos\beta + V_{90}(\tau)\sin\alpha\sin\beta\cos\theta \\ w_e &= V_{90}(\tau)\sin\alpha\sin\theta \end{aligned} \tag{2}$$

where

$$V_0(\tau) = \frac{(1-\tau^2)^{3/2}}{(1-\tau^2)^{1/2} - 1/2\,\tau^2\log[(1+\sqrt{1-\tau^2})/(1-\sqrt{1-\tau^2})]} \tag{3}$$

$$V_{90}(\tau) = \frac{2V_0(\tau)}{2V_0(\tau) - 1}$$

$$\cos\beta = \frac{(1-x^2)^{1/2}}{[1+x^2(\tau^2-1)]^{1/2}} \tag{4}$$

and α is a specified function of time, being constant in the present study. The configuration in the meridional plane is illustrated in figure 1 with S the stagnation point of the inviscid flow defined by $\theta = 0$, $x = -\{1-\tau^2\tan^2\alpha\}^{1/2}$.

Turning to the boundary layer we define $(u, w\sqrt{\nu}, w)$ to be the velocity components respectively along the meridional lines θ = const, along the normals to the spheroid and in the azimuthal direction where ν is the kinematic viscosity of the fluid and is assumed small. Then

$$\frac{\partial}{\partial x}(h_2 u) + \frac{\partial}{\partial \theta}(h_1 w) + \frac{\partial}{\partial y}(h_1 h_2 v) = 0 \tag{5}$$

$$\frac{\partial u}{\partial t} + \frac{u}{h_1}\frac{\partial u}{\partial x} + \frac{w}{h_2}\frac{\partial u}{\partial \theta} + v\frac{\partial u}{\partial y} + w^2 K_2 = -\frac{1}{h_1}\frac{\partial \hat{p}}{\partial x} + \frac{\partial^2 u}{\partial y^2} \tag{6}$$

$$\frac{\partial u}{\partial t} + \frac{u}{h_1}\frac{\partial w}{\partial x} + \frac{w}{h_2}\frac{\partial w}{\partial \theta} + v\frac{\partial w}{\partial y} - uwK_2 = -\frac{1}{h_2}\frac{\partial \hat{p}}{\partial \theta} + \frac{\partial^2 w}{\partial y^2} \tag{7}$$

where $y\sqrt{\nu}$ measures distance along the outward-drawn normal from the body,

$$h_1 = \left[\frac{1 + x^2(\tau^2 - 1)}{1 - x^2}\right]^{1/2}, \qquad h_2 = \tau(1 - x^2)^{1/2} \tag{8}$$

are the metric coefficients,

$$K_2 = \frac{x}{[1 + x^2(\tau^2 - 1)]^{1/2}(1 - x^2)^{1/2}} \tag{9}$$

is the geodesic curvature of the surface lines x = const, and $\hat{p}$ is the reduced pressure. The appropriate boundary conditions are

$$\begin{aligned} u = v = w = 0 \qquad & \text{at} \qquad y = 0 \\ u \to u_e, \quad w \to w_e \qquad & \text{as} \qquad y \to \infty \end{aligned} \tag{10a}$$

The specification of the problem is completed by assigning initial conditions on u,w with respect to space and time. The spatial conditions are that on the line of symmetry w = 0 and u vanishes for all y at that value of x for which $u_e = 0$. This is physically and mathematically sensible for impulsive problems in which the stagnation point is fixed but is not necessarily correct when the angle of attack is varying with time, see Cebeci and Carr (1981) for example. The temporal conditions are that at t = 0 both u and w vanish on the body y = 0 on the line of symmetry but are equal to their external values elsewhere. Thus

$$u = w = 0 \qquad \text{at} \qquad y = 0, \; t = 0 \quad \text{for all} \quad x \tag{10b}$$

while

$$u = u_e, \; w = w_e \qquad \text{for} \qquad y > 0, \; t = 0 \quad \text{and all } x.$$

In the early studies of the properties of the boundary layers on prolate spheroids conducted by Wang (1970) and Hirsh and Cebeci (1977), some difficulty was experienced in continuing the solution past the nose at $x = -1$, primarily because of the singularities in the properties of h_1, h_2 and K_2 there. A common procedure was first to perform the integration along the line of symmetry from the stagnation point to as near the nose as possible and then to jump across the nose to the same value of x on the leeside ($\theta = \pi$) assuming that the flow properties are essentially unchanged. After that integration on the leeside may be continued as far as separation. Afterwards the procedure may be extended to more general points in the neighborhood of the nose. This technique is effective at moderate values of τ [$\tau = 1$ corresponds to a sphere] but leads to difficulties as $\tau \to 0$ especially at high angles of attack. Cebeci et al. (1980) demonstrated that the singularity may be removed by a suitable transformation of the surface coordinate system enabling a smooth passage to be made around the nose. The transformation is equally effective for unsteady boundary layers and is now explained for the limiting case of a paraboloid which corresponds to $\tau = 0$.

The first step is to define new surface coordinates by

$$\frac{dS}{S} = \frac{h_1 dx}{h_2} = \frac{[1 + x^2(\tau^2 - 1)]^{1/2}}{\tau(1 - x^2)}\, dx$$

$$X = S\cos\theta, \qquad Z = S\sin\theta, \qquad Y = y/\tau \tag{11}$$

with $S = 0$ at $x = -1$, and new velocity components by

$$u = U\cos\theta + W\sin\theta, \qquad w = W\cos\theta - U\sin\theta, \qquad v = V/\tau \tag{12}$$

The purpose of this transformation is to convert the polar form of the equations (5) - (7) into a quasi-rectangular-Cartesian form which is free of singularities. The governing equations reduce to

$$N\left(\frac{\partial U}{\partial X} + \frac{\partial W}{\partial Z}\right) + \frac{\partial V}{\partial Y} - L(UX + WZ) = 0 \tag{13}$$

$$\frac{\partial U}{\partial t} + N\left(U\frac{\partial U}{\partial X} + W\frac{\partial U}{\partial Z}\right) + LW(WX - UZ) + V\frac{\partial U}{\partial Y} = \gamma\beta_1 + \frac{\partial^2 U}{\partial Y^2} \tag{14}$$

$$\frac{\partial W}{\partial t} + N\left(U\frac{\partial W}{\partial X} + W\frac{\partial W}{\partial Z}\right) - LU(WX - UZ) + V\frac{\partial W}{\partial Y} = \gamma\beta_2 + \frac{\partial^2 W}{\partial Y^2} \tag{15}$$

where $\gamma\beta_1$, $\gamma\beta_2$ are pressure-gradient parameters defined by the requirement that $u \to u_e$, $w \to w_e$ as $Y \to \infty$ and

$$N = \frac{S\tau^2}{h_2}, \qquad L = \frac{\tau^2}{S}\left(\frac{1}{h_2} + K_2\right) \tag{16}$$

For the paraboloid we let $\tau \to 0$ after defining

$$p = \frac{(1 - x^2)^{1/2}}{\tau} \tag{17}$$

when

$$S = \frac{p}{(1 + p^2)^{1/2} + 1}\exp\left[(1 + p^2)^{1/2} - 1\right] \tag{18}$$

$$N = \frac{S}{p}, \qquad L = \frac{(1 + p^2)^{1/2} - 1}{pS(1 + p^2)^{1/2}} \tag{19}$$

and so Eqs. (13) - (15) are independent of τ. We write (U_e, W_e) for the limits of $(u_e \cos\theta - w_e \sin\theta,\ u_e \sin\theta + w_e \cos\theta)$ as $\tau \to 0$ and then

$$U_e = \frac{pX\cos\alpha}{S(1 + p^2)^{1/2}} - 2\left(1 - \frac{pX^2L}{S}\right)\sin\alpha \tag{20}$$

$$W_e = \frac{pZ\cos\alpha}{S(1 + p^2)^{1/2}} + \frac{2XZLp}{S}\sin\alpha \tag{21}$$

so that

$$\gamma\beta_1 = N\left(U_e\frac{\partial U_e}{\partial X} + W_e\frac{\partial U_e}{\partial Z}\right) + LW_e(W_eX - U_eZ) \tag{22}$$

$$\gamma\beta_2 = N\left(U_e\frac{\partial W_e}{\partial X} + W_e\frac{\partial W_e}{\partial Z}\right) - LU_e(W_eX - U_eZ) \tag{23}$$

These equations are free of all geometric singularities and in particular at the nose p = 0. There is therefore now no special problems about integrating the equations through the nose although it should be noted that the equations are only appropriate at distances from it cor esponding to p = O(1). This is the natural length scale for the paraboloid but in terms of general thin axisymmetric bodies this distance is $O(\tau^2)$ from the nose.

2.1 Line-of-Symmetry Equations

These may be deduced from the general form Eq. (13) et seq. given in the previous section using similar arguments to those in Cebeci et al. (1981). We shall *not* repeat them in detail but merely state the transformations and the final form. First we write

$$U = U_0(X,Y,T) + O(Z^2), \qquad V = V_0(X,Y,T) + O(Z^2) \tag{24}$$

$$W = Z \exp[1 - \sqrt{1 + p^2}]W_1(X,Y,T) + O(Z^3) \tag{25}$$

and allow for negative values of X by permitting p to become negative. When p < 0 the sign of S in Eq. (18) must be changed and generally X = S sgnp in the limit Z → 0. On the leeside line of symmetry p < 0.

We now substitute Eqs. (24), (25) into (13) et seq and take the limit Z → 0. The external velocity components reduce to

$$U_{oe} = \frac{p\cos\alpha - 2\sin\alpha}{(1 + p^2)^{1/2}}, \qquad W_{1e} = \frac{[(1 + p^2)^{1/2} + 1]\cos\alpha + 2p\sin\alpha}{(1 + p^2)^{1/2}} \tag{26}$$

To put the equations into the most convenient form for numerical integration of the impulsive problem, with primes denoting differentiation with respect to n we write

$$n = \frac{Y}{(1 + p^2)^{1/4}t^{1/2}}, \quad \bar{V}_0 = t^{-1/2}(1 + p^2)^{1/4}V_0 - \frac{npt^{-1/2}}{2(1 + p^2)}U_0 \tag{27}$$

$$U_o = U_{oe} f' \quad , \qquad W_1 = g' \tag{28}$$

where f and g are functions of p,η,t. Then

$$\overline{V}_o = - U_{oe} \frac{\partial f}{\partial p} - f(a_1 U_{oe} + \frac{dU_{oe}}{dp}) - a_2 g \tag{29}$$

where

$$a_1 = \frac{p}{2(1 + p^2)} - \frac{p}{(p^2 + 1)^{1/2} + 1}, \qquad a_2 = \frac{(1 + p^2)^{1/2}}{1 + (1 + p^2)^{1/2}} \tag{30}$$

and the appropriate boundary conditions for f and g are:

$$\begin{aligned} &f = f' = g = g' = 0 \qquad \text{at} \qquad \eta = 0, \\ &f' \to 1, \qquad g' \to w_{1e} \qquad \text{as} \qquad \eta \to \infty \end{aligned} \tag{31}$$

The momentum equations reduce to

$$f''' + P_1 f f'' + P_6 g f'' + P_2[1 - (f')^2] + P_{13} \eta f'' = P_7 \frac{\partial f'}{\partial t} + P_{10}(f' \frac{\partial f'}{\partial p} - f'' \frac{\partial f}{\partial p}) \tag{32}$$

$$g''' + P_1 f g'' + P_6 g g'' + P_3 (f')^2 + P_4 (g')^2 + P_5 f' g' + P_{12} + P_{13} \eta g''$$

$$= P_7 \frac{\partial g'}{\partial t} + P_{10} (f' \frac{\partial g'}{\partial p} - g'' \frac{\partial f}{\partial p}) \tag{33}$$

where

$$\begin{aligned} &P_1 = t(a_1 U_{oe} + \frac{dU_{oe}}{dp}), \qquad P_2 = t \frac{dU_{oe}}{dp} \\ &P_3 = t U_{oe}^2, \quad P_4 = -t a_2, \quad P_5 = t a_3 U_{oe}, \quad P_6 = t a_2, \\ &P_7 = t(1 + p^2)^{1/2}, \quad P_{10} = t U_{oe}, \\ &P_{12} = t(U_{oe}^2 + a_2 W_{1e}^2 - a_3 U_{oe} W_{1e} + U_{oe} \frac{\partial W_{1e}}{\partial p}), \quad P_{13} = \frac{1}{2}(1 + p^2)^{1/2} \\ &a_3 = \frac{p}{(1 + p^2)^{1/2}} + \frac{p}{1 + (1 + p^2)^{1/2}} \end{aligned} \tag{34}$$

These two equations (32) and (33) are in a convenient form for numerical integration since at t = 0 f,g and their derivatives are given by

$$f = \eta \operatorname{erf}(\lambda\eta) - \frac{1}{\lambda\sqrt{\pi}}(1 - e^{-\lambda^2\eta^2}), \qquad g = W_{1e} f$$

$$f' = \operatorname{erf}(\lambda\eta), \qquad g' = W_{1e} f' \tag{35}$$

$$f'' = \frac{2\lambda}{\sqrt{\pi}}\, e^{-\lambda^2\eta^2}, \qquad g'' = W_{1e} f''$$

where

$$\lambda = \frac{1}{2}(1 + p^2)^{1/4}$$

Further, the integration in the direction p increasing may be assumed to start at the stagnation point p = 2 tanα, where f,g are independent of p and satisfy partial-differential equations in η,t only, and proceeds in a straightforward way since $U_{oe} > 0$ when p > 2 tanα. A similar remark applies to the integration in the direction of p decreasing since $U_{oe} < 0$ when p < 2 tanα.

3.0 SOLUTION PROCEDURE

The numerical solution of equations (32) and (33) was obtained using the Box method, a two-point finite-difference method developed by H. B. Keller and extensively used for two-dimensional flows, both steady and unsteady, and for three-dimensional steady flows. Here we use two versions of the Box method, the regular box in regions where $f' \geq 0$ across the layer and the zig-zag box in regions where f' < 0 at any value of η. Specifically in advancing the solution to a new value of t or p, this property of f' determined the choice of the box scheme. The details of the box scheme are described in Bradshaw et al. (1981).

Calculations of the unsteady boundary layers were carried out for angles of attack α of 30°, 40°, 45°, 50°. Provided separation did not occur, the solution of the equations by the regular box was appropriate, no numerical difficulties were encountered and the solution was smooth. The step-sizes chosen for all computations were $\Delta p = 0.2$, $\Delta t = 0.2$; in selected cases comparisons were made with studies using step-sizes of $\Delta p = 0.1$ and $\Delta t = 0.1$ or smaller and the differences were negligible. However, once separation occurred, the regular box became prone to instabilities and was replaced in this domain by the zig-zag box over all η and the step-sizes in p and t were reduced. Various calculations were carried out with a nonuniform mesh in p, t in the neighborhood of separation. The smallest value of Δp was 0.0005 near the separation point; the step size in t was progressively reduced as the calculations proceeded, the smallest value being 0.01. Elsewhere Δp was fixed at 0.2. Comparisons with solutions using larger step-sizes gave confidence that the results were reliable outside the separated region for $t < 7$, but that inside the separated region smaller step-sizes in p and t were necessary to avoid small oscillations which developed for $t > 5.5$ at $\alpha = 50°$.

4.0 RESULTS

The principal properties of the unsteady boundary layers are the skin-friction components defined by

$$U_0'(o,p,t) = t^{-1/2} U_{e_0} f''(o,p,t) = (1 + p^2)^{1/4} \left(\frac{\partial U_0}{\partial Y}\right)_w \qquad (36a)$$

$$W_1'(o,p,t) = t^{-1/2} g''(o,p,t) = (1 + p^2)^{1/4} \left(\frac{\partial W_1}{\partial Y}\right)_w \qquad (36b)$$

and the displacement thicknesses defined by

$$\Delta_1(p,t) = U_{e_0} t^{1/2} \lim_{\tau \to \infty} (\eta - f) = (1 + p^2)^{-1/4} \int_0^\infty (U_{eo} - U_o)dy \qquad (37a)$$

$$\Delta_2(p,t) = t^{1/2} \lim_{\eta \to \infty} [\eta W_{e_1} - g) = (1 + p^2)^{-1/4} \int_0^\infty (W_{e1} - W_1)dy \qquad (37b)$$

These are displayed in Fig. 2 for $\alpha = 30°$ when separation does not occur. In Fig. 3 we display the properties of U_o' for $\alpha = 40°$, a solution which is on the verge of separation, and in Fig. 4 we show all the functions [Eqs. (36) and 37] for $\alpha = 50°$ when separation clearly occurs. Where appropriate the corresponding steady-state results of Cebeci et al. (1980) are included in these graphs for comparison purposes.

The graphs show that for $p > 0$, i.e. on the windward line of symmetry, the steady-state solution is rapidly approached as t increases and is essentially established for $t > 1$.

For $p < 0$, i.e. on the leeward line of symmetry, the flow properties in the steady state have two interesting features. First for any value of α, the cross-flow displacement thickness Δ_2 rapidly decreases with p and soon becomes negative, even if separation has not occurred, and in fact is exponentially large and negative when p is large and negative. The unsteady data for $\alpha = 30°$, Fig. 2d, confirms this trend but the limits $t \to \infty$, $p \to \infty$ are not interchangeable, i.e. for any t the graph of Δ_2 flattens out for large enough -p and for any $p < -2$ the graph of Δ_2 eventually approaches the steady state.

Second the steady-state meridional component U_o' of the skin friction does not tend monotonically to a limit as $p \to -\infty$, but even at small values of α has a trough followed by a peak due to the overshoot in the external velocity (26). Further, at $\alpha > \alpha_c \doteq 41°$, U_o' actually vanishes at $p = p_c(\alpha)$, when p_c is a point near $p = -1$ depending on the particular choice of α. The solution is singular at this point and the calculation must terminate.

The unsteady solution approaches the steady state as $t \to \infty$ for $\alpha < \alpha_c$ (Figs. 2 and 3) but more slowly on the windward side. Some overshoot may occur but it is small and may be an indication of a fall-off in accuracy of either the steady-state or the unsteady solutions. For $\alpha > \alpha_c$ (Fig. 4), the same remarks apply as long as $p > p_c(\alpha)$ and flow reversal has not occurred. For smaller values of p, reversed flow occurs and there is no corresponding steady-state solution. If $\alpha = 45°$, separation first occurs at $t = 5.64$ when $p = -1.2$; it remains confined within the range $-1.0 > p > -1.4$ and is weak until $t = 6$ when the computation was terminated. It might be argued that W_1' and Δ_2 are approaching limit states as $t \to \infty$ but Δ_1 is definitely showing signs of a pronounced negative minimum near $p = -1.2$.

Separation is marginal for $\alpha = 45°$ and so a more extensive computation was carried out for $\alpha = 50°$. In this case separation set in when $t \approx 3.71$ at $p = -1.083$ and gradually spread out as t increased to extend around the range $-0.908 \leq p \leq -1.396$ at $t = 6$ when the calculations became somewhat dubious due to oscillations and instabilities, a behavior previously observed in relation to the circular cylinder started impulsively from rest, Cebeci (1982). Over the same range of t the variation of Δ_2 and W_1' may appear to remain smooth but U_0' and Δ_1 develop sharp minima just downstream from separation.

5.0 THE SINGULARITY?

We now investigate whether the results obtained for $\alpha = 50°$ allow us to conclude that when the computation terminated the flow properties are consistent with a singularity centered just downstream of separation in the neighborhood of $t = 6$.

Two possible structures for a terminating singularity to the solution have been proposed of which one is due to Smith (1982). In his model, the

viscous terms are significant at breakdown, which is a generalization of the Goldstein singularity, and both skin-friction and displacement thickness are infinite. No example of such a structure has yet been found and although we cannot rule out its relevance in the present flow, our inclination is to prefer the second possibility, due to van Dommelen and Shen (1982a), in which the skin friction remains finite while the displacement thickness becomes infinite. A full description of this, the van Dommelen and Shen (1982b) singularity, has not yet been given and some questions are still open but strong evidence in favor of its being appropriate to an unsteady boundary layer on a circular cylinder has been provided by van Dommelen and Shen themselves and by Cowley (1983) and Ingham (1983) and on an oscillating airfoil by Cebeci et al. (1983).

The essence of the singularity is inviscid and independent of the pressure gradient. Thus, in the case of a two-dimensional boundary layer, with equations

$$\frac{\partial u}{\partial x} + \frac{\partial v}{\partial y} = 0, \tag{38a}$$

$$\frac{\partial u}{\partial t} + u\frac{\partial u}{\partial x} + v\frac{\partial u}{\partial y} = -\frac{1}{\rho}\frac{\partial p}{\partial x} + \frac{\partial^2 u}{\partial y^2}, \tag{38b}$$

let us suppose the singularity is centered at $t = t_0$, $x = x_0$. Then in its simplest form we write

$$u = -u_0 + (t_0 - t)^{1/2}\,\tilde{u}(\tilde{x},\tilde{y}) \tag{39}$$

when $0 < t_0 - t \ll 1$, $|x - x_0| \ll 1$,

where

$$\tilde{x} = [(x - x_0) - u_0(t_0 - t)]/(t_0 - t)^{3/2}, \quad \tilde{y} = y(t_0 - t)^{1/4}$$

and the determination of $\tilde{u}$ reduces to quadratures. This structure must be matched to other structures near $y = 0$ and as $y \to \infty$ but the principal gross

features can be inferred from (39). The displacement thickness has a peak at $\tilde{x} = 0$ which becomes infinite like $(t_0 - t)^{-1/4}$ as $t \to t_0$. On the other hand, the skin friction remains finite as $t \to t_s$ for all x. The velocity profile becomes very flat as $t \to t_0$ provided $\tilde{x} \sim 1$, with $u = -u_0$ over a length $(t_0 - t)^{-1/4}$ normal to the surface, the adjustment to the boundary conditions both on the surface and at infinity taking place over effectively finite ranges of values of y. Further details of the structure of the singularity, on the basis of a Lagrangian representation may be found in van Dommelen's thesis (1981) and in Elliot, et al. (1983) on the basis of an Eulerian representation as exemplied by (38).

This theory may be adapted to our problem at least in principle. We replace u,x,y in (39) by f',p,n and neglect the left-hand side of (32) in the neighborhood of $p = p_0$, $t = t_0$. Then the equation for $\tilde{f}'$ is the same as that for $\tilde{u}$ and we may infer that f' is as likely to develop the van Dommelen and Shen singularity as is u in the circular cylinder problem. Thus the displacement thickness Δ_1 can be expected to develop an increasingly sharp peak at a value of p which is a linear function of t and at a finite line, a needle-like infinity. Also, the corresponding component of skin friction U_0' remains finite and smooth.

The evidence in Fig. 4 supports these conclusions. A more severe test is to plot the streamwise displacement velocity, $\partial\Delta_1/\partial p$, as a function of p for various t and this is done in Fig. 5a after smoothing the data for $p < -0.95$. It is convenient to compare these graphs with one (Fig. 6) kindly provided by Cowley for solution of (38) with $u_e = \sin x$, in which the singularity occurs at $t \simeq 3.0$. The similarities in form are striking; the principal difference being a slight drift in $\min_p \partial\Delta_1/\partial p$ away from separation as t increases in contrast to the prediction in (39) [$u_0 > 0$]. The value of $\min_p \Delta_1$ drifts towards the separation point. Further the more detailed plots of U_0' in Fig. 5b confirm the smooth behavior of this function.

If now we examine (33) we see that the same form for g' may be assumed provided g_0' is taken equal to f_0' and again the left-hand side of (33) may be neglected. This means that Δ_2 should also develop a needle-like singularity and Fig. 4d shows no evidence of this. However, plots of $\partial\Delta_2/\partial p$ as functions of p for various t, displayed in Fig. 5c, show clear signs of the development of a strong minimum, similar to Fig. 6, which does drift towards separation. The alternative possibility that Δ_2 is finite seems to require that as η increases g' has reached the value W_{1e} before the inviscid zone $\eta \approx 1$ is reached. Were this the case, the two sides of (33) would not balance over this zone since then $f' \approx f_0' \neq 1$.

6.0 DISCUSSION

In this paper we have examined the evolution of the unsteady boundary layer on the line of symmetry of a paraboloid which is set, impulsively, into motion at $t = 0$ with uniform velocity and at an angle α of attack. We have shown that if $\alpha < \alpha_c$ ($\approx 41°$) and the steady-state boundary layer exists everywhere on this line, the unsteady solution approaches it reasonably quickly and without any significant special features. The same is true for $\alpha > \alpha_c$ on the windward side. On the leeward side, the steady-state boundary layer separates and the solution must terminate there because the external pressure gradient is fixed. The unsteady boundary layer is initially unseparated but develops a region of reversed flow after a finite time. A short time later the first displacement thickness Δ_1 develops a pronounced peak and we advance arguments for believing that this is associated with an incipient singularity which terminates the calculation.

The results obtained here are also relevant to other bodies, most obviously prolate spheroids but others as well. Our earlier studies demonstrated that in the neighborhood of the nose, the governing equations for a spheroid can be

transformed into a form in which the paraboloid equations appear as a natural limit ($\tau \to 0$, see Eq. (17)) in which the various parameters of the flow remain finite. Hence we may confidently expect that any special feature, such as separation, which appears in the one will also appear in the other. Wang and Fan (1982) have studied the unsteady boundary on a prolate spheroid for $\alpha = 45°$ (the value of τ was not supplied). They found that whereas the steady-state boundary layer separated at $p = 0.39/\tau$, the unsteady boundary layer does not separate for any finite t. This result we regard as being in direct conflict with ours and moreover a matter of surprise. For not only does a small nonzero τ make very little difference to our form of the equations, but the result is hard to understand in the general context of boundary-layer theory. At present the discrepancy is inexplicable. The choice of coordinate systems for integration around the nose does seem to be very cumbersome and it would be interesting to repeat the calculations using the system advocated here. For the purposes of this discussion we shall set this calculation at one side.

We repeat, therefore, that in our view the phenomena we have discussed in connection with the paraboloid would also appear in a comparable study of prolate spheroids. In particular the singularity would appear after a finite time in an integration of the unsteady equations on the line of symmetry in the neighborhood of the nose and just downstream of separation if $\alpha > \alpha_c$. Generalization of this conclusion to the unsteady boundary layer over the whole spheroid is of interest. In principle the integration of four dimensional boundary-layer equations (x,θ,y,t) wavelike with respect to (x,θ,t) using the Keller-box scheme is no more difficult than those for steady two-dimensional flow, provided we make the appropriate modifications to account for the varying direction of flow across the boundary layer. It just takes longer because there are more mesh points to consider in the (x,θ,t) space.

We may expect that the solution of these equations will develop a singularity on the normals to a curve C on the spheroid after a finite time, the precise time varying from point to point of C, and it will be inviscid in character. Indeed van Dommelen and Shen (1982b) (see also Cowley 1982) have suggested a generalization of their two-dimensional structures which seems likely to be appropriate. From our experience with two-dimensional unsteady boundary layers we are confident that the Keller-box scheme can carry the integration up to the first onset of the singularity. It remains to be seen whether the calculation can be extended beyond this time and over what part of the flowfield - certainly the front portion of the body can be treated but the precise boundaries are presumably fixed by an application of the Raetz (1957) theory of influence-regions.

Finally, it is of interest to consider the possible impact of this study on the calculation of steady boundary layers on bodies of revolution. The extensive computations in τ on prolate spheroids showed that on the windward part of the separation line the flowfield develops a Goldstein-Brown (1965) singularity. On the leeside of the ok of accessibility (Cebeci et al. 1981b), the calculations for large α in general must be terminated by the external streamline through the ok, so that the question of the structures of the leeside separation line is irrelevant. At small values of α ($\simeq 6°$) this limitation does not apply but nevertheless the computation breaks down. It is believed that this breakdown occurs very near leeside separation but a reconciliation with the Goldstein-Brown structure was not achieved. In particular, the blowing velocity is <u>negative</u> whereas the theory requires it to be large positive.

A feature of the singularity is that when $t_0 - t$ is small (39), the blowing velocity is large and positive as $x \to x_0$ and after peaking becomes negative in order to bring the displacement thickness back to more moderate

values. Thus there is some parallel here with the leeside separation. Further encouragement to this notion comes from the structure, Eq. (39), which suggests that in the central regime of the singularity, the velocity components are almost constant. If this is the case, in the leeside separation singularity the governing equations for steady three-dimensional and unsteady two- dimensional boundary-layer flow are effectively the same and so the assumption of a van Dommelen and Shen singularity is as consistent for the one class as the other.

The boundary layer on a paraboloid at incidence is of interest in connection with this line of thought. For with $\alpha < \alpha_c$, its structure when $p \gg 1$ has much in common with that of the unsteady boundary layer on a circular cylinder, both on the leeside line of symmetry and on the windward side. In comparing the two we must relate p to t and the cross-flow velocity on the paraboloid to the external velocity on the circular cylinder and perhaps we should not push the analogy too far in the reversed flow regime on the circular cylinder. The unsteady boundary-layer separates at $\theta \approx 106°$ when t is large and the solution is regular there. The same will be true for the steady problem but it remains to be seen whether a singularity occurs in the neighborhood of $\theta = 106°$ at finite p. It is tempting to conjecture that the boundary layer will also breakdown somewhere near $\theta = 111°$ with a singularity at a finite value of p, and that further downstream there will be a region of inaccessibility, spreading out in both directions of θ and terminating at $\theta = 106°$ and $\theta = \pi$ as $p \to \infty$, just as occurs with the ok at higher angles of attack.

5.0 ACKNOWLEDGMENT

This research was supported under Air Force Office of Scientific Research contract F49620-82-C-0055 and under the National Science Foundation Grant No. MEA-8018565.

6.0 REFERENCES

Bradshaw, P., Cebeci, T. and Whitelaw, J.H. (1981) Engineering Calculation Methods for Turbulent Flows. Academic Press, London.

Brown, S.N. (1965) Singularities Associated with Separating Boundary Layers. Phil. Trans. Roy. Soc. London A 257, 409-444.

Carr, L. W. and McAlister, K.W. (1983) The Effect of a Leading-Edge Slat on the Dynamic Stall of an Oscillating Airfoil. AIAA Paper 83-2533.

Carr, L.W., McAlister, K.W. and McCroskey, W.J. (1977) Analysis of the Development of Dynamic Stall Based on Oscillating Airfoil Experiments. NASA TN D-8382.

Cebeci, T. (1979) The Laminar Boundary Layer on a Circular Cylinder Started Impulsively From Rest. J. Comp. Phys. 31, 153-172.

Cebeci, T. (1982) Unsteady Separation. In Numerical and Physical Aspects of Aerodynamic Flows, (ed. T. Cebeci) Springer-Verlag, NY, 265-277.

Cebeci, T. and Carr, L.W. (1981) Prediction of Boundary-Layer Characteristics of an Oscillating Airfoil. In Unsteady Turbulent Shear Flows, (ed. R. Michel, J. Cousteix and R. Houdeville), Springer-Verlag, 145-158.

Cebeci, T. and Carr, L.W. (1983) Calculation of Boundary Layers Near the Stagnation Point of an Oscillating Airfoil. NASA TM 84305.

Cebeci, T., Khattab, A.A. and Stewartson, K. (1980) On Nose Separation. J. Fluid Mech, 97, p. 435-454.

Cebeci, T., Stewartson, K. and Williams, P.G. (1981a) Separation and Reattachment Near the Leading Edge of a Thin Airfoil at Incidence. AGARD Conf. Proceedings 291, Paper No. 20.

Cebeci, T., Khattab, A.A. and Stewartson, K. (1981b) Three-Dimensional Laminar Boundary Layers and the Ok of Accessibility. J. Fluid Mech, 107, p. 57-87.

Cebeci, T., Khattab, A.A. and Schimke, S.M. (1983) Can the Singularity be Removed in Time-Dependent Flow? A.F. Workshop, Colorado Springs, CO.

Cousteix, J., Houdeville, R. and Janelle, J. (1981) Response of a Turbulent Boundary Layer to a Pulsation of the External Flow With and Without Adverse Pressure Gradient. In Unsteady Turbulent Shear Flows (ed. R. Michel, J. Cousteix, R. Houdeville) Springer-Verlag, 120-144.

Cowley, S.J. (1982) On Unsteady Three-Dimensional Laminar Boundary-Layer Separation. Submitted for publication.

Cowley, S. (1983) Private communication.

Davis, S.S. and Malcolm, G.N. (1980) Experimental Unsteady Aerodynamics of Conventional and Supercritical Airfoils. NASA TM 81221.

Dowell, E.H., Bland, S.R. and Williams, M.H. (1981) Linear/Nonlinear Behavior in Unsteady Transonic Aerodynamics. AIAA Paper 81-643.

Elliott, J.W., Cowley, S.J. and Smith, F.T. (1983) Breakdown of Boundary Layers: (i) On Moving Surfaces; (ii) in Semisimilar Unsteady Flow; (iii) in Fully Unsteady Flow. Submitted to Geophysical and Astrophysical Fluid Dynamics.

Geissler, W. (1983) Theoretical and Experimental Dynamic Stall, Investigations on a Rotor Tip Blade. Second Symposium on Numerical and Physical Aspects of Aerodynamic Flows, Long Beach, CA.

Hirsh, R.S. and Cebeci, T. (1977) Calculation of Three-Dimensional Boundary Layers with Negative Cross-Flow on Bodies of Revolution. AIAA Paper No. 77-683.

Ingham, D.B. (1983) Unsteady Separation. Submitted to J. Comp. Phys.

McCroskey, W.J. (1982) Unsteady Airfoils. Ann. Rev. Fluid Mech. 14, 285.

McCroskey, W.J., McAlister, K.W., Carr, L.W. and Pucci, S.L. (1982) An Experimental Study of Dynamic Stall on Advanced Airfoil Sections 1, 2, 3. NASA TM-84245.

Mehta, U. (1977) Dynamic Stall of an Oscillating Airfoil. AGARD Conf. Proceedings No. 227, Paper No. 23.

Raetz, G. S. (1957) A Method of Calculating Three-Dimensional Boundary Layers of Steady Compressible Flows. Northrop Corp. Rept. No. NA158-73.

Shamroth, S.J. (1981) A Turbulent Flow Navier-Stokes Analysis for an Airfoil Oscillating in Pitch. In Unsteady Turbulent Shear Flows. (ed. R. Michel, J. Cousteix, R. Houdeville), 185-196.

Smith, F.T. (1982) On the High Reynolds Number Theory of Laminar Flows. IMA Journal Appl. Mech. 28, 207-281.

Telionis, D.P. (1979) Review. Unsteady Boundary Layers, Separated and Attached. J. Fluids Engrg. 101, 29-43.

Telionis, D.P. and Tsahalis, D.T. (1974) Unsteady Laminar Separation Over Cylinder Started Impulsively from Rest. Acta Astronautica 1, 1487.

van Dommelen, L.L. (1981) Ph.D. Thesis, Cornell University.

van Dommelen, L.L. and Shen, S.F. (1982a) The Genesis of Separation. In Numerical and Physical Aspects of Aerodynamic Flows, (ed. T. Cebeci) Springer-Verlag, NY, 293-311.

van Dommelen, L.L. and Shen, S.F. (1982b) Boundary Layer Separation Singularities as Stationary Points in Lagrangian Space. Submitted for publication.

Wang, K.C. (1970) Three-Dimensional Boundary Layer Near the Plane of Symmetry of a Spheroid at Incidence. J. Fluid Mech., 43, p. 187-209.

Wang, K.C. (1976) Separation of Three-Dimensional Flow. In Viscous Flow Symp. Lockheed-Georgia Co., Atlanta, Georgia.

Wang, K.C. and Fan, Z.Q. (1982) Unsteady Symmetry-Plane Boundary Layer and 3-D Unsteady Separation. Part I. High Incidence. San Diego State University Rept. AEOEM TR-82-01.

Williams, J.C. (1977) Incompressible Boundary-Layer Separation. Ann. Rev. Fluid Mech. 9, 119.

Williams, J.C. (1982) Flow Development in the Vicinity of the Sharp Trailing Edge on Bodies Impulsively Set into Motion. J. Fluid Mech. 115, 27-37.

Williams, J.C. and Stewartson, K. (1983) Flow Development in the Vicinity of the Sharp Trailing Edge on Bodies Impulsively Set into Motion. Part 2, J. Fluid Mech. 131, 177.

Young, W.H., Jr. (1982) Fluid-Mechanics Mechanisms in the Stall Process of Airfoils for Helicopters. In Numerical and Physical Aspects of Aerodynamic Flows (ed. T. Cebeci), 601-615.

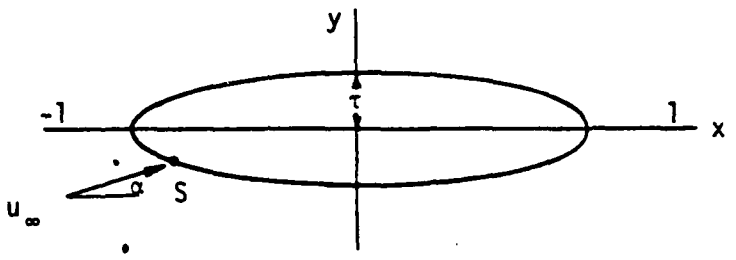

Figure 1. Notation for prolate spheroid.

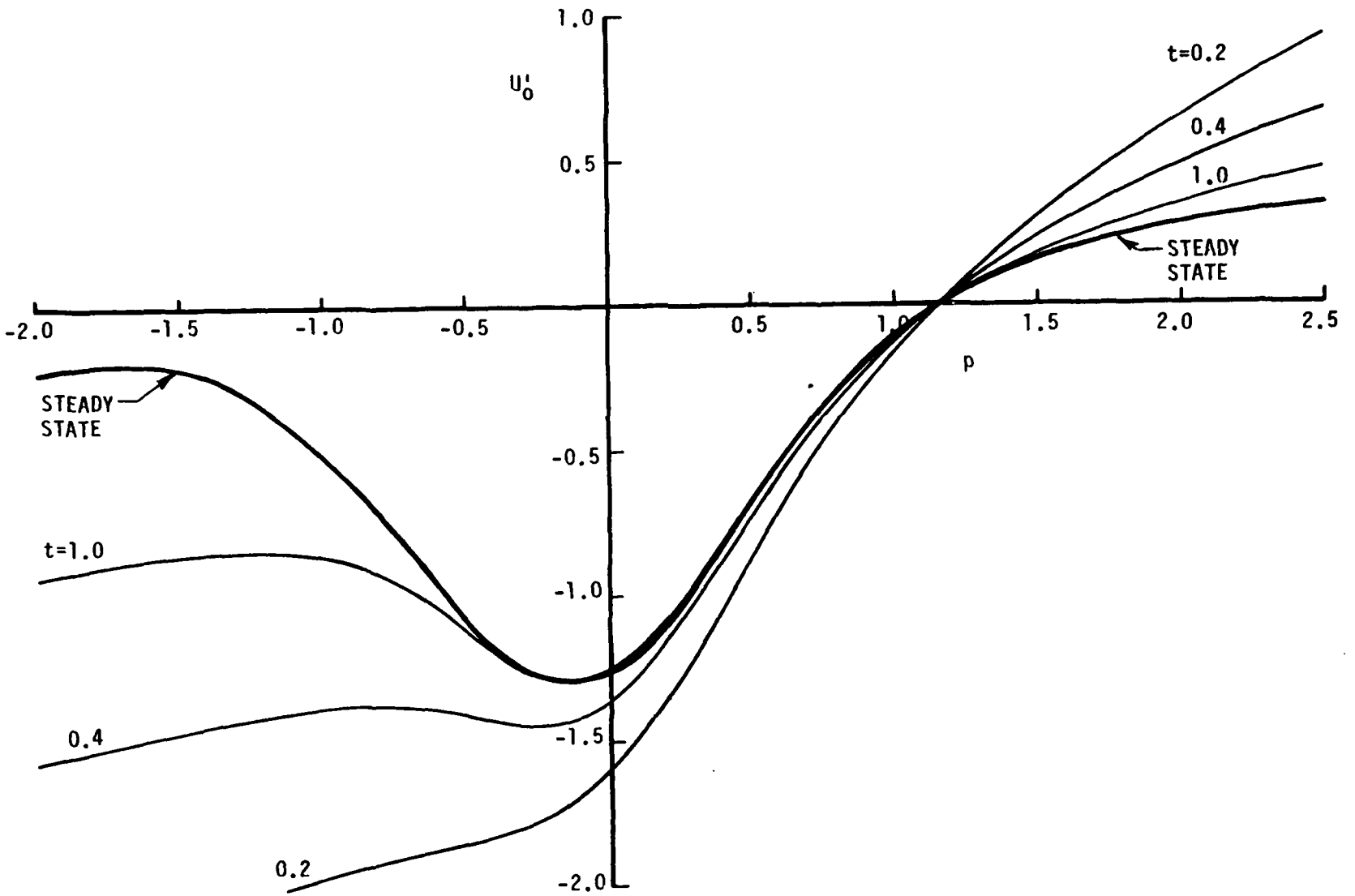

Figure 2. Variation of skin-friction components and displacement thicknesses with p and t for $\alpha = 30°$. (a) Streamwise skin-friction component.

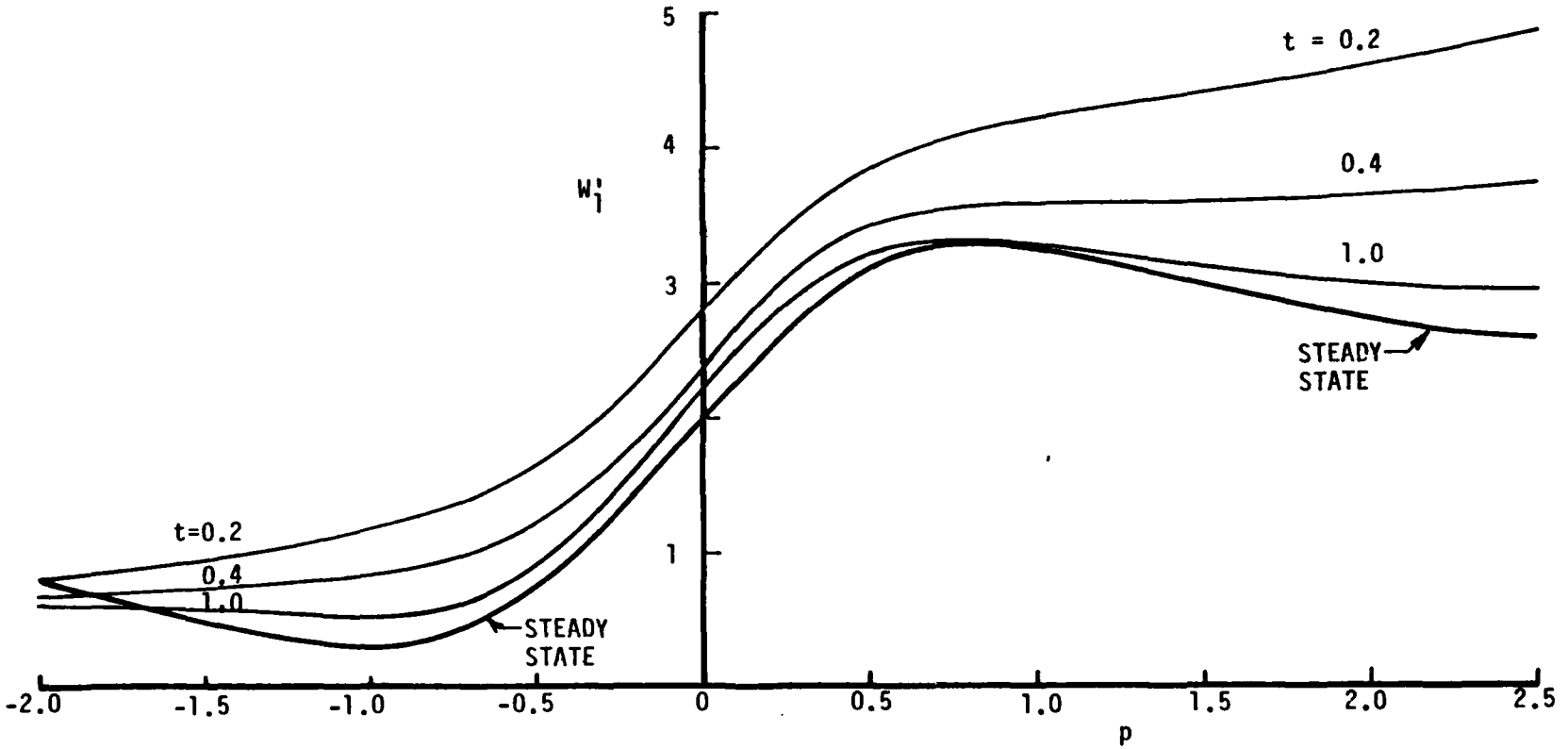

Figure 2. (b) Circumferential skin-friction component.

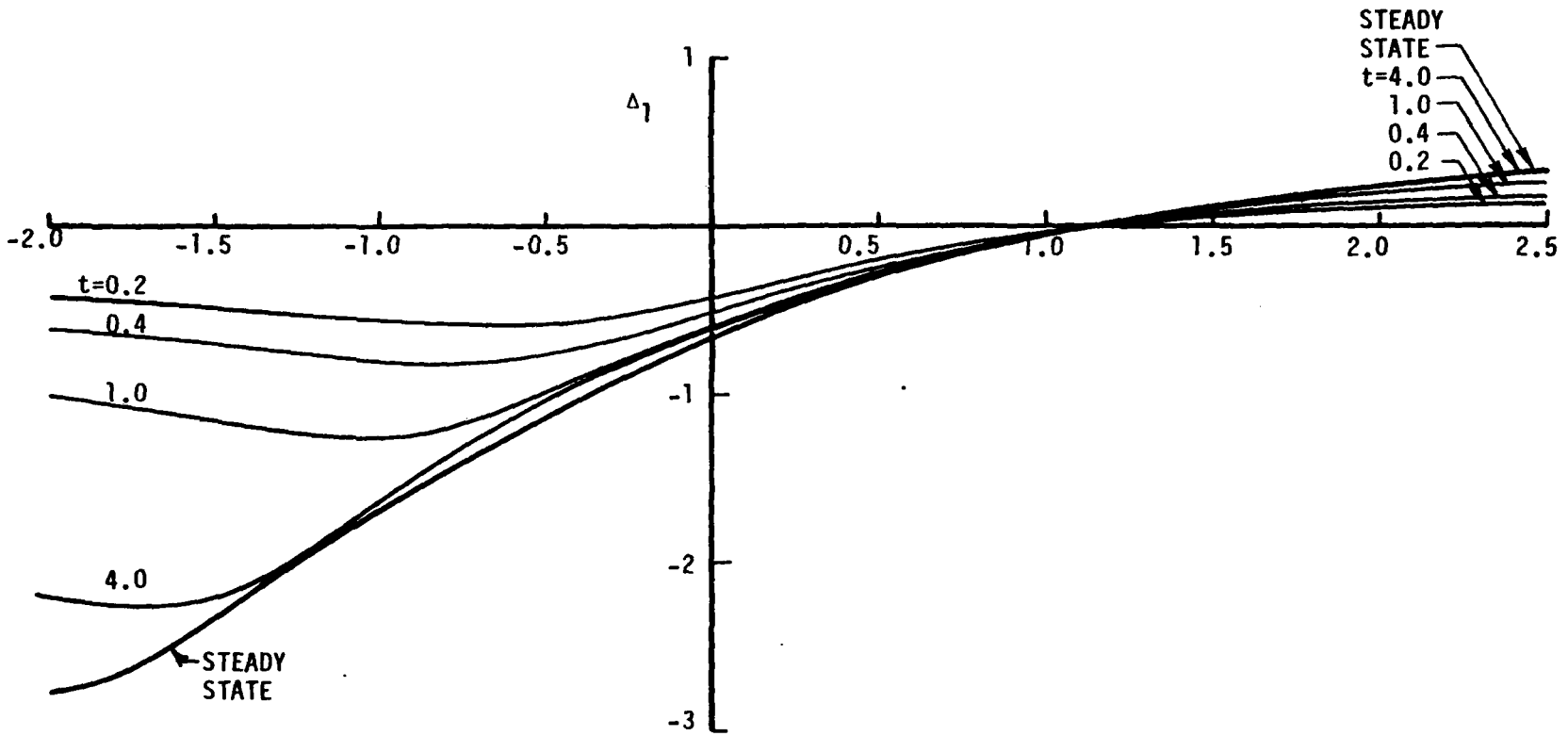

Figure 2. (c) Streamwise displacement thickness.

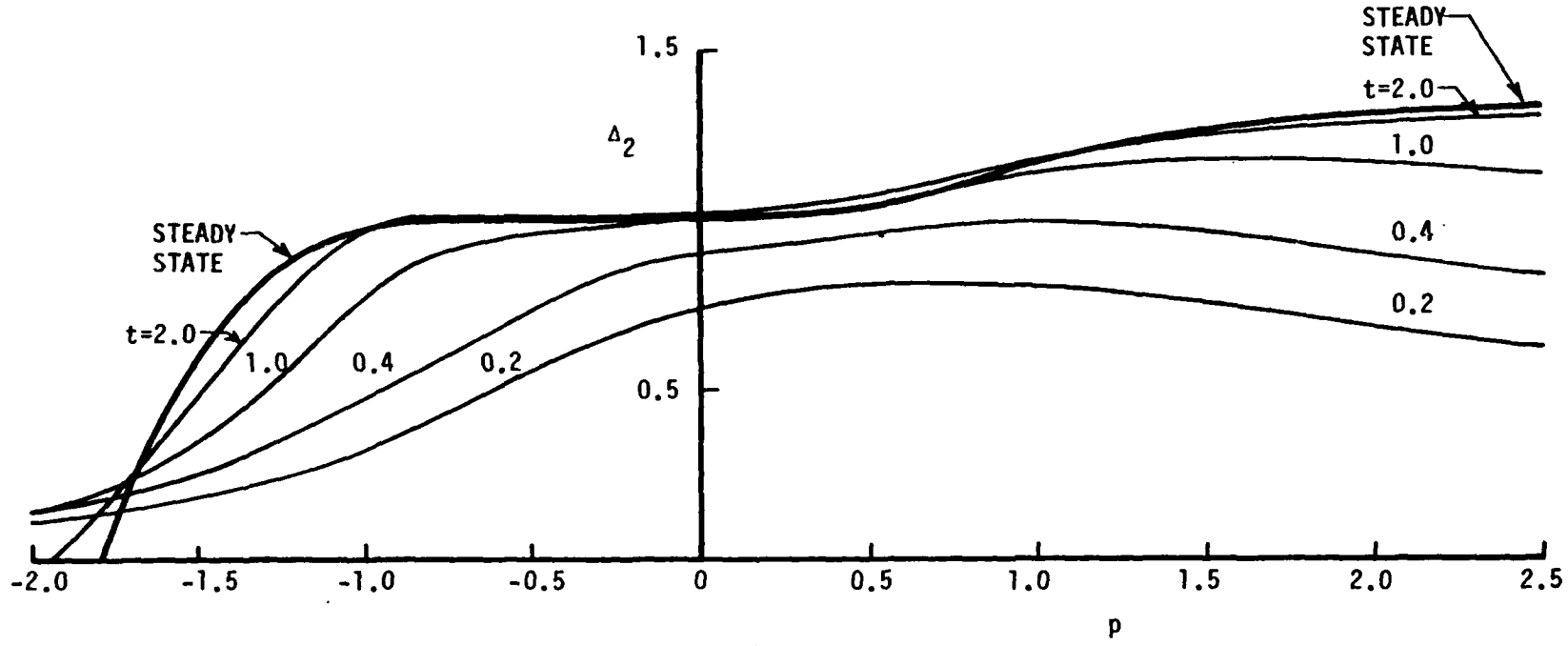

Figure 2. (d) Circumferential displacement thickness.

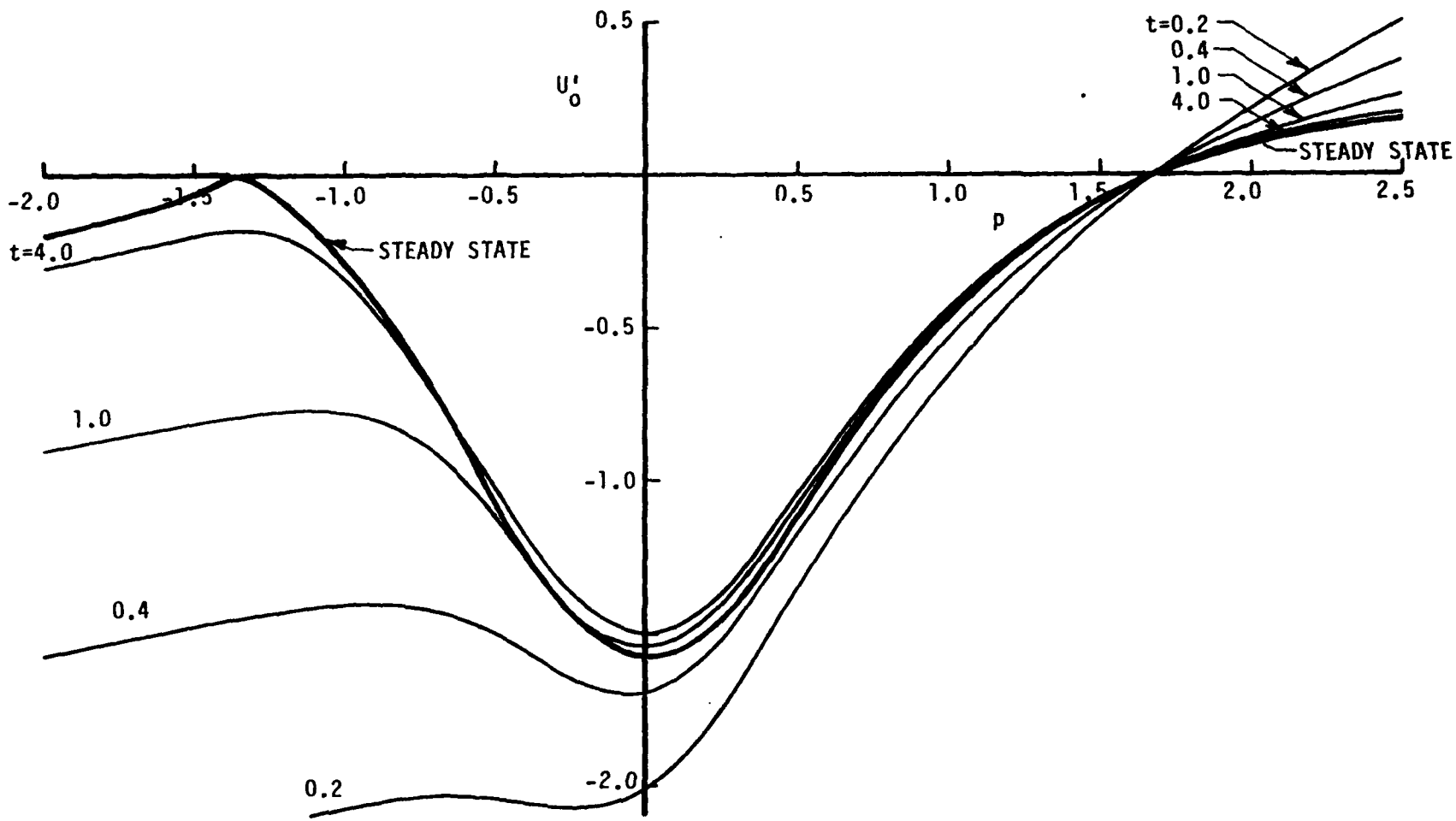

Figure 3. Variation of streamwise skin-friction component U_0' with p and t for $\alpha = 40°$.

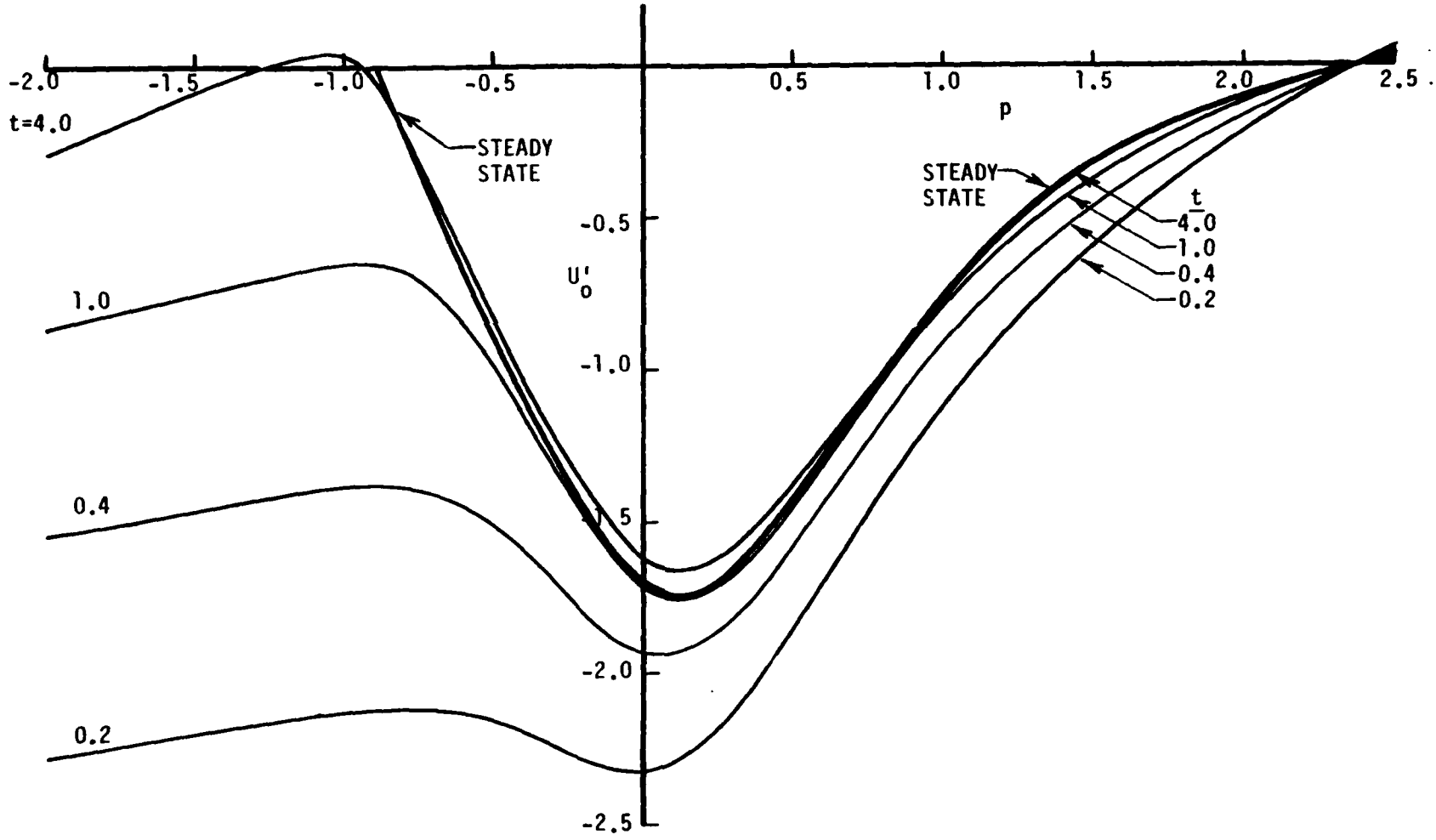

Figure 4. Variation of skin-friction components and displacement thicknesses with p and t for $\alpha = 50°$. (a) Streamwise skin-friction component.

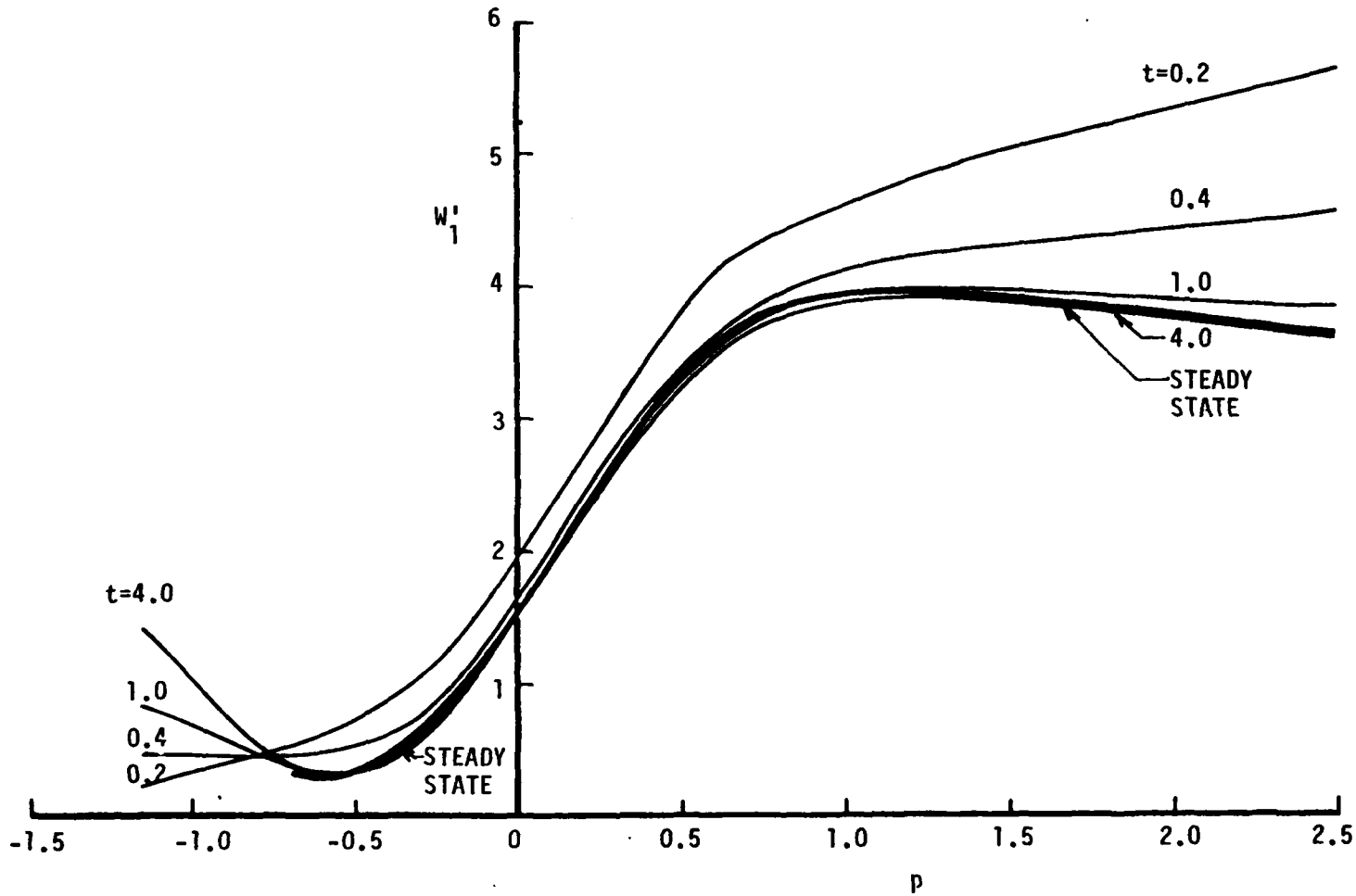

Figure 4. (b) Circumferential skin-friction component.

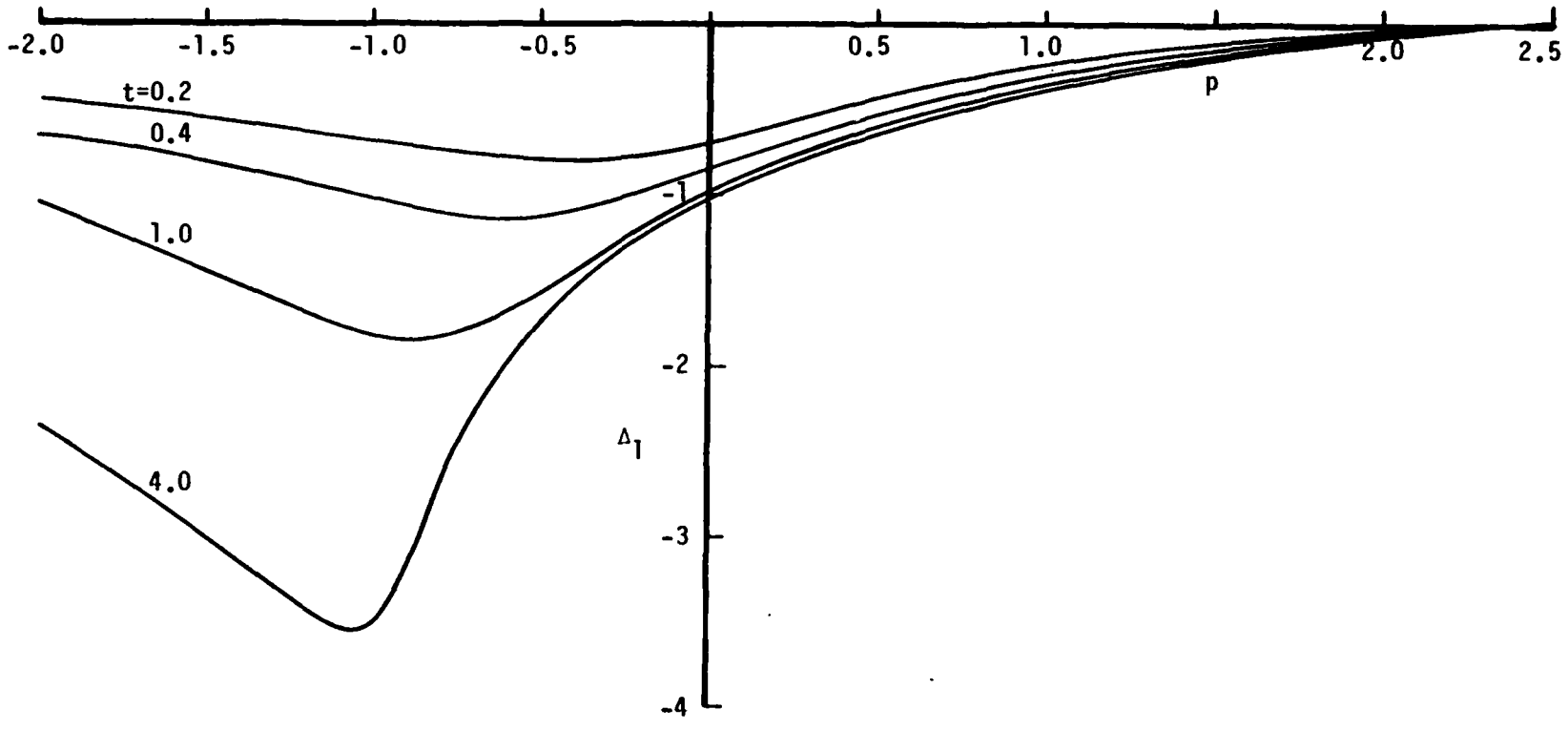

Figure 4. (c) Streamwise displacement thickness.

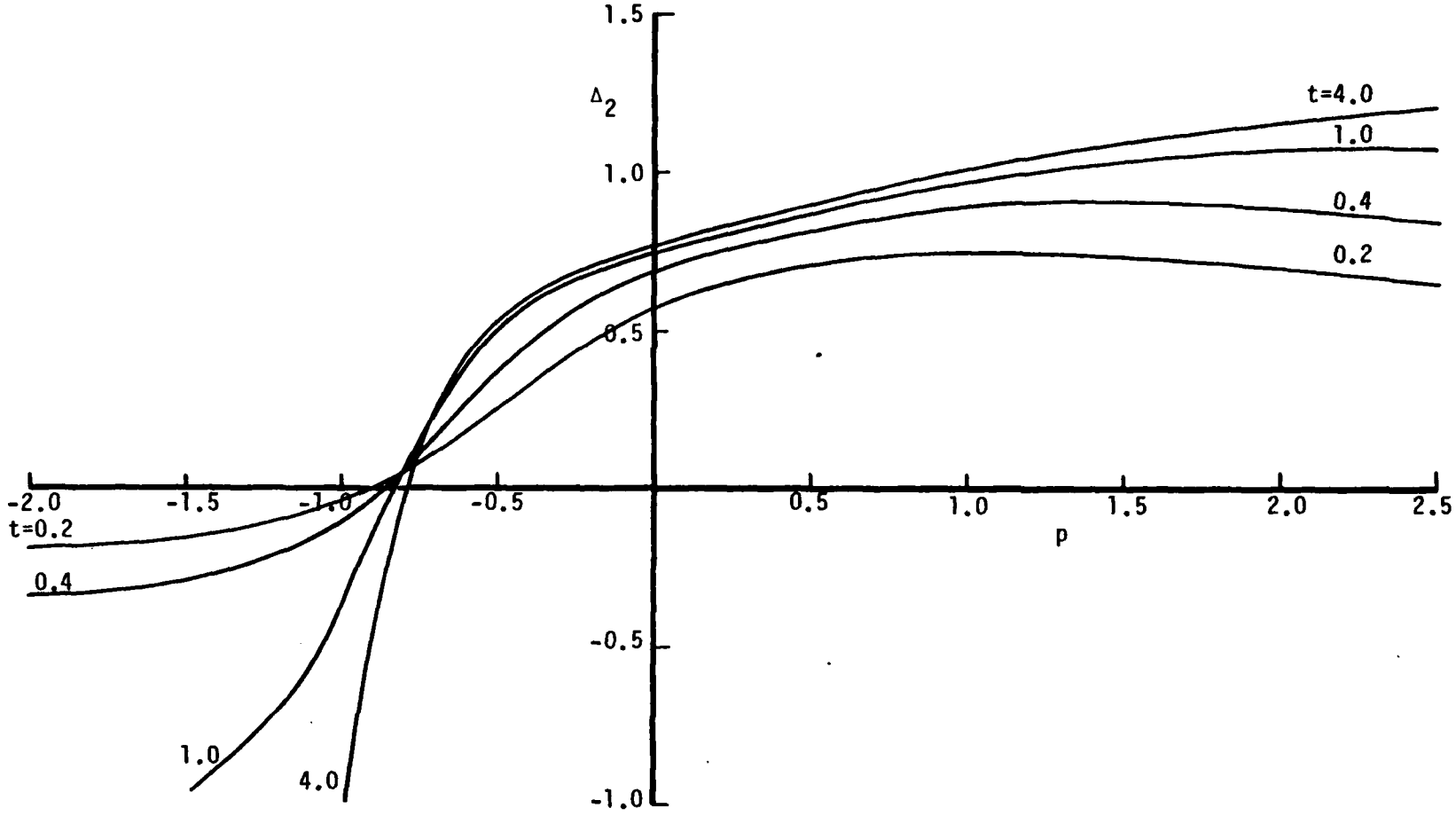

Figure 4. (d) Circumferential displacement thickness.

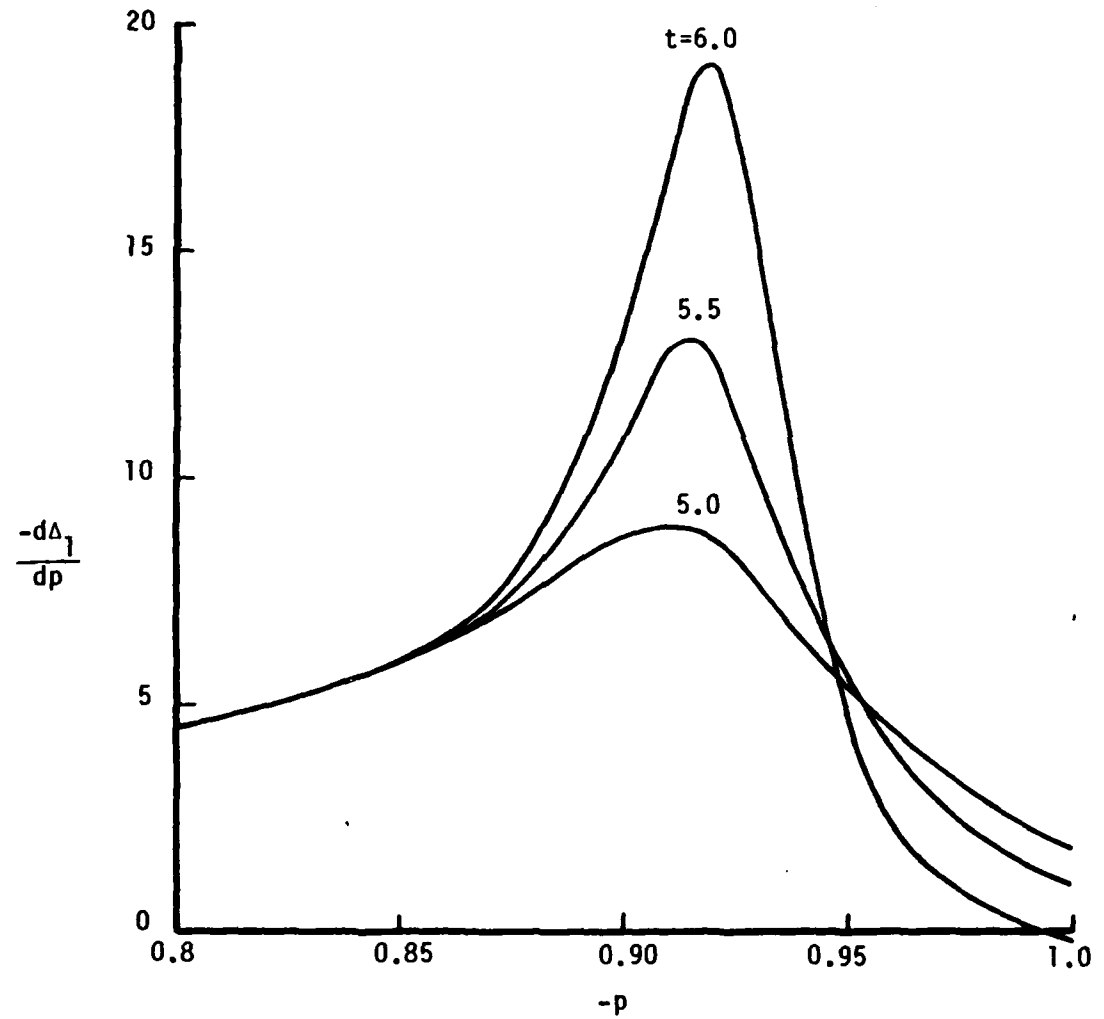

Figure 5. Computed results for α = 50°. (a) Streamwise displacement velocity.

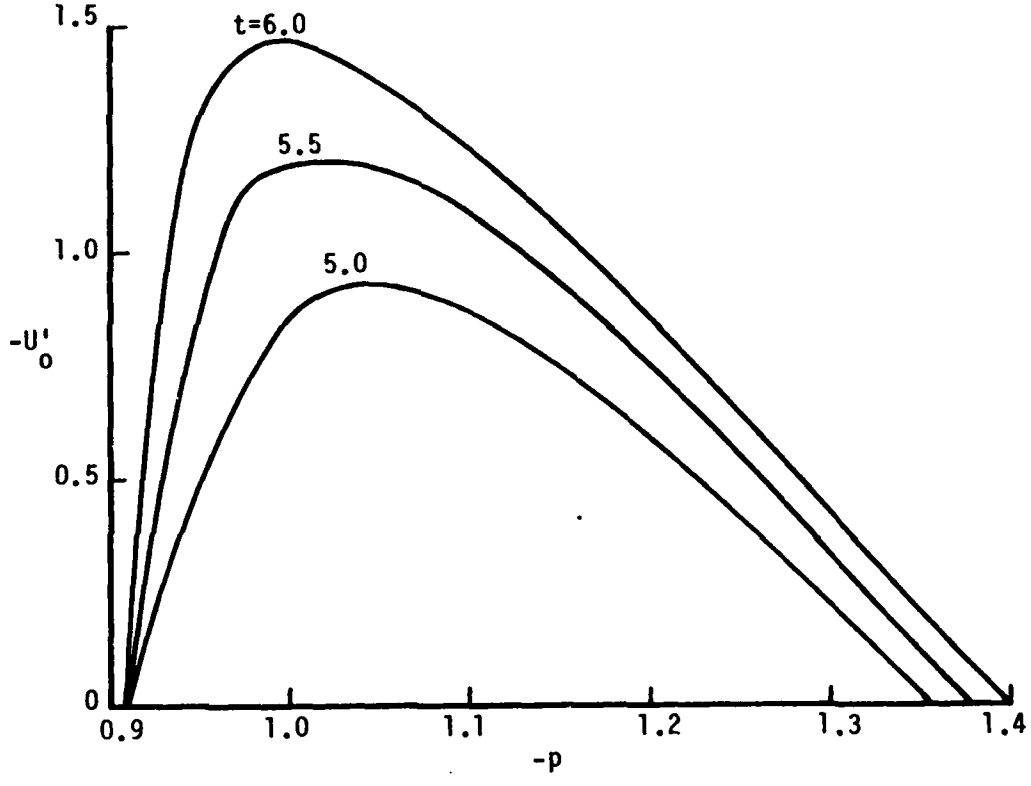

Figure 5. (b) Streamwise skin-friction component.

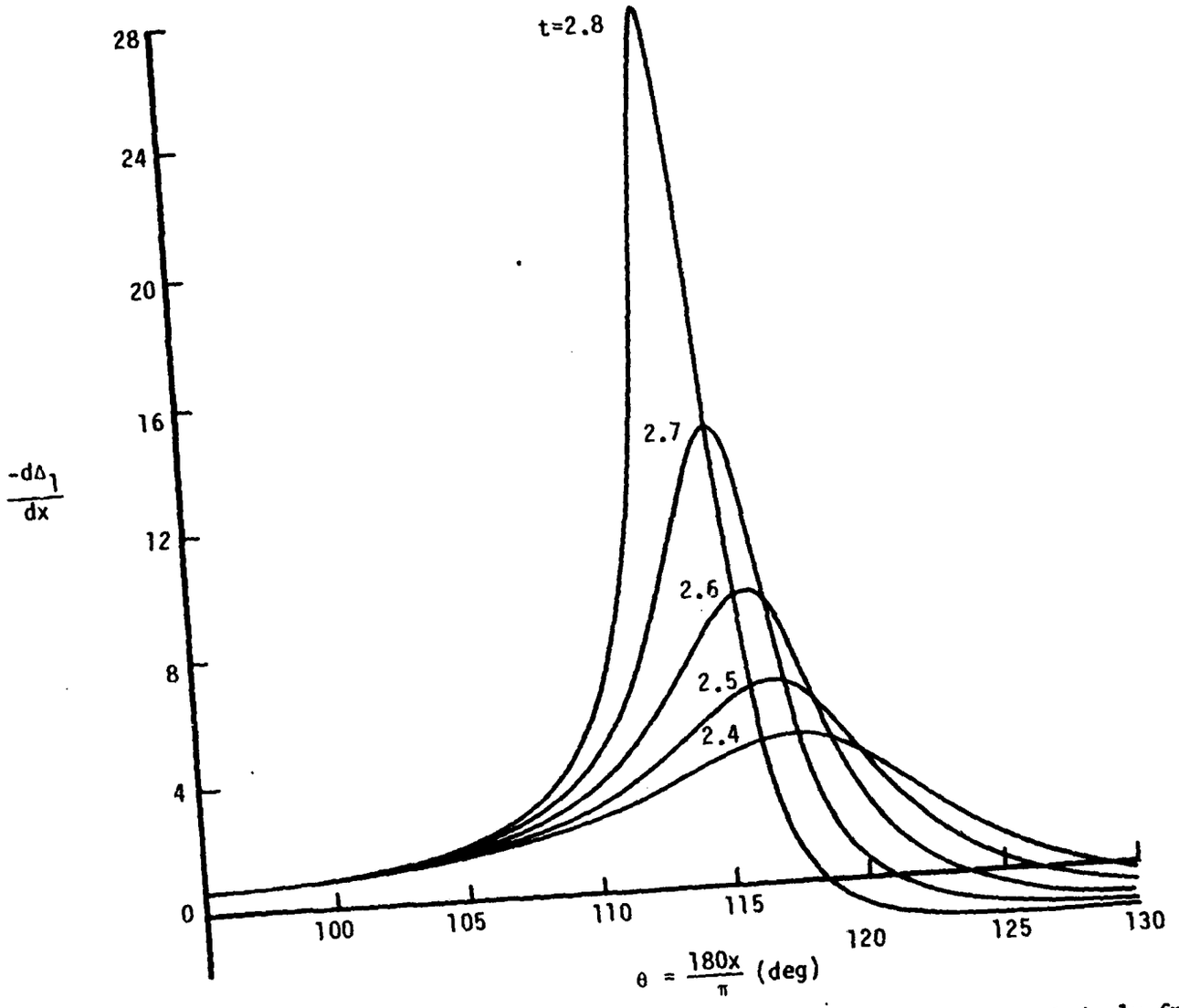

Figure 6. Variation of displacement velocity for the circular cylinder started impulsively from rest. Calculations are due to Cowley (1983).


DATE
ILME